Synthesis and Characterization of Vanadyl Phosphite, $V^{IV}OHP^{III}O_3 \cdot 1.5H_2O$

V. V. Guliants,† J. B. Benziger,*,‡ and S. Sundaresan‡

Departments of Chemistry and Chemical Engineering, Princeton University, Princeton, New Jersey 08544

Received January 3, 1995. Revised Manuscript Received May 16, 1995⊗

Vanadyl(IV) phosphite, $VOHPO_3 \cdot 1.5H_2O$, was synthesized by reduction of V_2O_5 in refluxing alcohol solutions (ethyl, isopropyl, and isobutyl alcohols) with subsequent addition of H_3PO_3. X-ray diffraction suggests an orthorhombic space group. Magnetic susceptibility data indicate the presence of exchange coupled vanadyl dimers associated with face-shared vanadyl octahedra similar to vanadyl hydrogen phosphate hemihydrate, $VOHPO_4 \cdot 0.5H_2O$. Vanadyl(IV) phosphite is a layered solid with an interlayer spacing of 7.27 Å. *n*-Alkylamines intercalated into the layered structure as single or double layers depending on the amine-to-host ratio, and the interlayer spacings, *d* (Å), increased linearly with the carbon number, n_c, as $d = 7.72 + 0.85n_c$ (monolayers), and $d = 6.49 + 1.82n_c$ (bilayers).

Introduction

The discovery of vanadium–phosphorus–oxide systems as a catalyst for selective oxidation of *n*-butane to maleic anhydride has prompted research into the synthesis of new vanadium phosphate phases. The most selective partial oxidation catalysts have been associated with vanadyl(IV) pyrophosphate, $(VO)_2P_2O_7$, formed by the dehydration of vanadyl(IV) hydrogen phosphate hemihydrate, $VOHPO_4 \cdot 0.5H_2O$. The crystalline structure of these phases is governed by the tendency of vanadium(IV) to form short vanadyl bonds resulting in distorted octahedral or square pyramidal geometries. Various approaches to prepare these and other vanadium phosphates have been reported that exploit easy interconversion of different oxidation states of vanadium.[1–4] Reductive intercalation approaches have been used with the layered vanadyl(V) orthophosphate dihydrate, $VOPO_4 \cdot 2H_2O$, to produce layered mixed V(IV)–V(V) phosphates with intercalated cations.[1,2] Oxidative deintercalation of some V(III) phosphates has produced NASICON-type V(IV) phosphates.[3] Solid state and hydrothermal methods have also been employed to produce a variety of layered and ribbon-type V(IV) phosphates.[4,5a,b] Haushalter and Zubieta et al.[5] have recently reported a number of new vanadium phosphates and arsenates displaying a variety of V–P(As)–O connectivities. They reported new layered A^{n+}–V^{III}/V^{IV} phosphates[5a,b] with the stair-step layer structure[5a] which consists of infinite ribbons six polyhedra in width and octahedral–tetrahedral framework reminiscent of $VOPO_4 \cdot 2H_2O$ structure type.[5b] The first example of 3-D chiral inorganic double helix has been synthesized in an effort to create vanadium phosphate solids combining the shape-selective adsorptivities of a zeolite with the thermal stability and reactive site of a catalytically active transition-metal oxide.[5c] Haushalter and Zubieta et al. have recently reported the hydrothermal synthesis and structural characterization of a new templated-layered V^{IV}=O organophosphonate,[5d] a mixed V^{IV}/V^{V} hydrogen phosphate with a one-dimensional $-V^{IV}-O-V^{V}-$ chains of corner-sharing VO_6 octahedra,[5e] a diaminobutane-intercalated layered system with distorted and defected $VOPO_4$ layers,[5f] $(NH_4)VOPO_4$ containing one-dimensional chains of VO_6 octahedra,[5g] and a V^{IV} phosphate containing corner-sharing V^{IV} square pyramids, phosphate tetrahedra, and incorporating propanediammonium dications.[5h]

Johnson and co-workers synthesized a class of layered V(IV) organophosphonates and organoarsenates with the general formula VOR (P or As)O_3·S, where R is an alkyl or other organo group, and S is a solvent molecule.[6] When the alkyl group R is methyl, ethyl, or propyl, these compounds have a layered structure similar to $VOHPO_4 \cdot 0.5H_2O$. For a larger R group, such as phenyl, linear V=O···V=O chains are connected through corners by the RPO_3 tetrahedra forming a layered solid with the phenyl groups pointed toward the interlayer space. The

† Department of Chemistry.
‡ Department of Chemical Engineering.
⊗ Abstract published in *Advance ACS Abstracts,* June 15, 1995.

(1) (a) Johnson, J. W.; Jacobson, A. J. *Angew. Chem., Int. Ed. Engl.* **1983**, *22*, 412. (b) Wang, S. L.; Kang, H. Y.; Chen, C. Y.; Lii, K. H. *Inorg. Chem.* **1991**, *30*, 3496.
(2) Matsubayashi, G.; Nakajima, H. *Chem. Lett.* **1993**, 31.
(3) Gopalakrishnan, J.; Rangan, K. K. *Chem. Mater.* **1992**, *4*, 745.
(4) (a) Huan, G.; Johnson, J. W.; Jacobson, A. J.; Corcoran, E. W., Jr.; Goshorn, D. P. *J. Solid State Chem.* **1991**, *93*, 514. (b) Lii, K. H.; Mao, L. F. *J. Solid State Chem.* **1992**, *96*, 436. (c) Lii, K. H.; Chueh, B. R.; Kang, H. Y.; Wang, S. L. *J. Solid State Chem.* **1992**, *99*, 72.
(5) (a) Haushalter, R. C.; Wang, Z.; Thompson, M. E.; Zubieta, J.; O'Connor, C. J. *Inorg. Chem.* **1993**, *32*, 3966. (b) Haushalter, R. C.; Wang, Z.; Thompson, M. E.; Zubieta, J. *Inorg. Chem.* **1993**, *32*, 3700. (c) Soghomonian, V.; Chen, Q.; Haushalter, R. C.; Zubieta, J.; O'Connor, C. J. *Science* **1993**, *259*, 1596. (d) Ishaque, K. M.; Lee, Y.-S.; O'Connor, C. J.; Haushalter, R. C.; Zubieta, J. *Inorg. Chem.* **1994**, *33*, 3855. (e) Haushalter, R. C.; Wang, Z.; Thompson, M. E.; Zubieta, J.; O'Connor, C. J. *J. Solid State Chem.* **1994**, *109*, 259. (f) Soghomonian, V.; Haushalter, R. C.; Chen, Q.; Zubieta, J. *Inorg. Chem.* **1994**, *33*, 1700. (g) Haushalter, R. C.; Chen, Q.; Soghomonian, V.; Zubieta, J.; O'Connor, C. J. *J. Solid State Chem.* **1994**, *108*, 128. (h) Soghomonian, V.; Chen, Q.; Haushalter, R. C.; Zubieta, J. *Chem. Mater.* **1993**, *5*, 1595.
(6) (a) Johnson, J. W.; Jacobson, A. J.; Brody, J. F.; Lewandowski, J. T. *Inorg. Chem.* **1984**, *23*, 3842. (b) Johnson, J. W.; Jacobson, A. J. EP 134157 A2, 1985. (c) Jacobson, A. J.; Johnson, J. W. *Mater. Sci. Monogr., 28A (React. Solids, Pt. A)* **1985**, 469. (d) Johnson, J. W.; Jacobson, A. J.; Butler, W. M.; Rosenthal, S. E.; Brody, J. F.; Lewandowski, J. T. *J. Am. Chem. Soc.* **1989**, *111*, 381. (e) Huan, G.; Jacobson, A. J.; Johnson, J. W.; Concoran, E. W., Jr. *Chem. Mater.* **1990**, *2*, 91. (f) Johnson, J. W.; Brody, J. F.; Alexander, R. M. *Chem. Mater.* **1990**, *2*, 198. (g) Huan, G.; Johnson, J. W.; Jacobson, A. J.; Merola, J. S. *J. Solid State Chem.* **1990**, *89*, 220.

0897-4756/95/2807-1485$09.00/0

Table 1. Elemental Composition of Vanadyl Phosphite $VOHPO_3 \cdot 1.5H_2O$ with Different Synthesis P/V Ratios

	calcd	$(P/V)_{init}$ = 1.00	$(P/V)_{init}$ = 1.17	$(P/V)_{init}$ = 1.30
V, %	29.29	27.21	28.26	27.01
P, %	17.81	14.02	15.93	18.87
H, %	2.32	2.37	2.76	1.90
H_2O, %	14.96	16.07	16.30	12.89
C, %	0	1.04	0.77	0.87
$(P/V)_{bulk}$	1	0.85	0.93	1.15
xH_2O (TGA)	1.5	1.70	1.75	1.64
(H_2O/V)bulk	1.5	1.67	1.63	1.35
$(O/P)_{XPS}$		4.3	4.3	4.2
$(P/V)_{XPS}$	1	1.54	1.57	1.59
P(2p), eV		133.6	133.4	133.4

structural similarity of the small alkyl group vanadyl(IV) phosphonates and $VOHPO_4 \cdot 0.5H_2O$ suggested that this class of compounds might provide a new synthesis route to an active vanadyl pyrophosphate catalyst. However, vanadyl(IV) phosphite, the first member of the $VORPO_3 \cdot S$ family with the alkyl group replaced by a hydrogen atom, i.e., R = H, has not been yet reported.

We report here the synthesis and characterization of a layered vanadyl(IV) phosphite compound, $VOHPO_3 \cdot 1.5H_2O$. The layered structure of vanadyl phosphite is confirmed by the formation of intercalated compounds with *n*-alkylamines. Vanadyl(IV) phosphite is the precursor to vanadyl pyrophosphate catalysts with high surface area (ca. 45 m^2/g) and selectivity to maleic anhydride in *n*-butane partial oxidation comparable to the conventional unpromoted catalyst.[7]

Experimental Section

Synthesis. Typically, vanadium pentoxide (5 g, Aldrich) was refluxed in anhydrous ethanol (100 mL, Aldrich) for 16 h. During this period of time the color of the suspended solid changed from V_2O_5 orange to light olive green. Phosphorous acid (Aldrich) dissolved in anhydrous ethanol (40 mL) was added to give a P/V ratio of 1.0−1.3 and the reaction mixture was refluxed for another 20 h. A light blue solid was separated by filtration, washed with ethanol and acetone, and dried in air. Elemental analysis shown in Table 1 was consistent with the formula $VOHPO_3 \cdot 1.5H_2O$.

$VOHPO_3 \cdot 1.5H_2O$ was also synthesized using a V(IV) source, such as vanadyl(IV) acetylacetonate or $VO(acac)_2$. In such experiment, 5 g of $VO(acac)_2$ (Aldrich) was added to phosphorous acid (P/V = 1.2) dissolved in anhydrous ethanol and refluxed for 2 days. The light blue solid was separated by filtration, washed with ethanol and acetone, and dried in air.

Intercalation of primary *n*-alkylamines was carried out by titrating 1 g of vanadyl phosphite suspended in 20 cm^3 of anhydrous *N,N*-dimethylacetamide at room temperature with 0.1 M standard solution of amines in *N,N*-dimethylacetamide at the equilibrium point in dry nitrogen atmosphere.

Characterization. Powder X-ray diffraction patterns were recorded with Scintag/USA DMS 2000 diffractometer using a Cu Kα radiation. The Raman spectra were obtained with a Spectra-Physics Ar^+ laser (Model 171) by using ca. 25−50 mW of the 514.5-nm line for excitation. About 100−200 mg of the powdered solid was pressed into a thin wafer about 1 mm thick with KBr backing for support. The sample was then mounted onto a spinning sample holder and rotated at ca. 2000 rpm to avoid local heating effects. A 90° collection geometry was employed to collect the scattered light. Infrared spectra were recorded on Nicolet 730 FTIR spectrometer using KBr disk technique. Powdered vanadyl phosphite was pressed into a pellet (7 mm diameter, 1 mm thick) under 3000 psi for magnetic susceptibility measurements. The XRD pattern of the pellet was identical to the powdered solid. Magnetic susceptibility data were collected on SQUID magnetometer (Quantum Design, MPMS system) with the pellet C_2 axis parallel to magnetic field H = 6.35 kG. Magnetization (M) isotherms collected at 20, 100, and 295 K were linear in the applied magnetic fields (H) of 2−8 kG and the saturation magnetization arising from the ferromagnetic impurities was found to be negligibly small. Thermogravimetric analysis of the intercalated phases was performed in air on a Perkin-Elmer TGS-2 thermal analyzer. BET surface areas were measured by nitrogen adsorption on a Quantachrome Quantasorb system. Elemental microanalysis of the solids was performed by Robertson Microlit Laboratories, Madison, NJ.

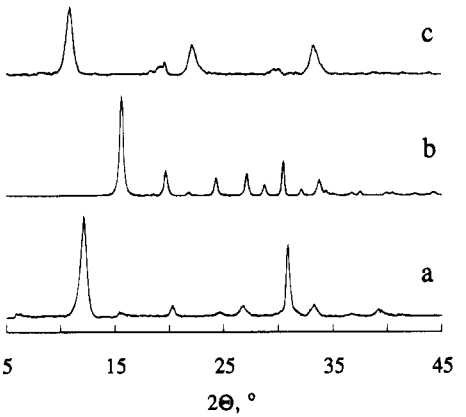

Figure 1. X-ray diffraction patterns of (a) vanadyl(IV) phosphite as crystallized from ethanol, (b) $VOHPO_4 \cdot 0.5H_2O$, and (c) vanadyl phosphite as crystallized in benzyl alcohol.

Results

The elemental analysis of the vanadyl phosphite samples synthesized at different P/V ratios is summarized in Table 1. Water content was determined by Karl Fischer method at room temperature and compared to the value calculated from the total weight loss by TGA in air at 1073 K according to the stoichiometric oxidation of $VOHPO_3 \cdot xH_2O$ into $VOPO_4$ (vide infra). Hydrogen content was determined by difference of total water after combustion and the water analysis at room temperature. Carbon content was determined from the amount of CO_2 evolved after combustion. Vanadium and phosphorus were determined by an ICP method.

The elemental analysis is consistent with a formula of vanadyl phosphite, $VOHPO_3 \cdot 1.5H_2O$, although the agreement is not exact. The material was synthesized as a powder with surface areas of 13−20 m^2/g. For a surface area of 20 m^2/g, the surface could adsorb up to 10 mol % water. Differences in termination of the surface with phosphite or vanadyl groups may also contribute a variation to the P/V ratio in the solid. X-ray photoelectron spectroscopy (XPS) of the sample showed a P(2p) binding energy of 133.4 eV, consistent with a P^{III} species.[8] This P(2p) binding energy is 0.6−0.7 eV lower than observed for P(V) species, e.g., in $VOHPO_4 \cdot 0.5H_2O$.[9] The XPS data also suggest surface enrichment of phosphorus, which is common to most vanadium phosphate catalysts.[9]

The XRD pattern of vanadyl phosphite synthesized in ethanol is shown in Figure 1a. The pattern is similar

(7) Guliants, V. V.; Benziger, J. B.; Sundaresan, S.; Wachs, I. E. Submitted to *Chem. Mater.*

(8) Moulder, J. F.; Stickle, W. F.; Sobol, P. E.; Bomben, K. D. *Handbook of X-ray Photoelectron Spectroscopy*; Chastain, J. , Ed. , Perkin-Elmer Corp.: Eden Prairie, MN, 1992.

(9) Zazhigalov, V. A.; Haber, J.; Stoch, J.; Pyatnitskaya, A. I.; Komashko, G. A.; Belousov, V. M. *Appl. Catal. A* **1993**, *96*, 135.

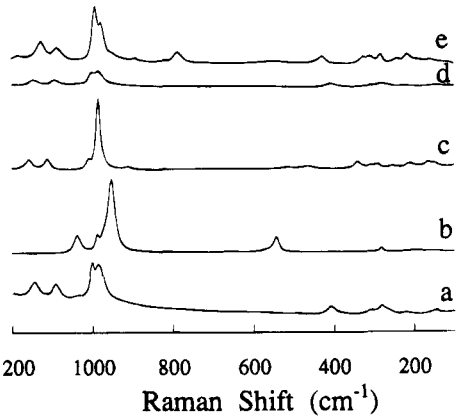

Figure 2. Raman spectra of (a) $VOHPO_3 \cdot 1.5H_2O$, (b) $VOPO_4 \cdot 2H_2O$, (c) $VOHPO_4 \cdot 0.5H_2O$, (d) $VOHPO_3 \cdot 1.5H_2O$ prepared from $VO(acac)_2$, (e) vanadyl methylphosphonate.

Table 2. Raman and IR Peaks of Vanadyl Phosphite at Room Temperature[a]

Raman (cm^{-1})	1146 M, 1093 M, 1042 W, 1001 vS, 985 vS, 407 M, 306 W, 282 M, 222 W, 147 W
IR (cm^{-1})	3583 W sh, 3539 S, 3365 S br, 3225 S br, 2963 sh, 2867 sh, 2439 vS, 1949 W br, 1617 vS, 1468 W, 1396 M sh, 1384 S, 1177 vS, 1081 vS, 1036 vS, 1010 vS, 964 vS, 811 S, 698 W, 630 sh br, 561 vS, 472 sh, 451 sh, 407 S, 376 S

[a] Labels: vS = very strong, S = strong, M = medium, W = weak, sh = shoulder, br = broad.

to that obtained for $VOHPO_4 \cdot 0.5H_2O$ (Figure 1b) except the interlayer spacing is larger in vanadyl phosphite (7.27 vs 5.69 Å). The structure of vanadyl phosphite depends on the nature of the solvent used during its crystallization. When benzyl alcohol was used, another crystal structure resulted as evidenced by the different XRD pattern shown in Figure 1c. Unfortunately, we have not been able to obtain vanadyl phosphite crystals of sufficient quality for single-crystal structural analysis. We have employed other chemical and physical characterization techniques to elucidate the structure of vanadyl phosphite.

The Raman spectrum of vanadyl phosphite is shown in Figure 2a. Raman spectroscopy has been widely recognized as a very sensitive characterization technique for metal oxides[10] and V(IV) and V(V) phosphates.[11] Raman spectrum of vanadyl phosphite (Figure 2a and Table 2) shows the bands at 1146 and 1093 cm^{-1} corresponding to both symmetric and asymmetric P–O stretching modes. The weak band at 1042 cm^{-1} apparently corresponds to the P–H stretching mode. The band at 1001 cm^{-1} is tentatively assigned to the vanadyl bond stretching mode which is expected in the 990–1000 cm^{-1} range based on the average bond length of 1.58 Å.[11,12] Another symmetric P–O stretching mode is at 985 cm^{-1}, whereas the coupled bending P–O and V–O vibration is observed at 410 cm^{-1}. The bands situated below 300 cm^{-1} correspond to skeletal vibrations of VO_6 and HPO_3 groups.

Phosphorous acid is a well-known reducing agent for V(V) which oxidizes it into orthophosphate species to produce $VOHPO_4 \cdot 0.5H_2O$.[13] As a result, both $VOPO_4 \cdot 2H_2O$ and $VOHPO_4 \cdot 0.5H_2O$ may be expected as impurities in the synthesis of vanadyl phosphite:

$$V_2O_5 + H_3PO_3 = 2VO_2 + H_3PO_4 \quad (1)$$

$$VO_2 + H_3PO_4 = VOHPO_4 \cdot 0.5H_2O + 0.5H_2O \quad (2)$$

$$V_2O_5 + 2H_3PO_4 + H_2O = VOPO_4 \cdot 2H_2O \quad (3)$$

Their Raman spectra are shown in Figure 2b,c, respectively. Vanadyl orthophosphate dihydrate has a characteristic high intensity P–O stretch at 953 cm^{-1} which is clearly absent in the spectrum of vanadyl phosphite. The Raman spectrum of $VOHPO_4 \cdot 0.5H_2O$ shown in Figure 2c is indicative of only one P–O stretching mode of moderate intensity at 988 cm^{-1}. To eliminate the ambiguity regarding the role of V(V) species, vanadyl phosphite has been prepared by reacting vanadyl(IV) acetylacetonate, $VO(acac)_2$, with phosphorous acid in ethanol under reflux. We have found that the 985 cm^{-1} band was still present in the spectrum of vanadyl phosphite synthesized according to the acetylacetonate method (Figure 2d). The spectra of the "V_2O_5" and "$VO(acac)_2$" samples of vanadyl phosphite are identical, the lower intensity of the spectrum of the latter being explained by its lower crystallinity observed in the powder XRD pattern.

Raman spectroscopy may also be useful in establishing local structural similarities between analogous compounds. The Raman spectra of vanadyl phosphite and the next member of the phosphonate family, vanadyl methylphosphonate are shown in Figure 2a,e, respectively. Vanadyl methylphosphonate was prepared by the method described by Johnson et al.[6a] The spectra exhibit a number of similar features, such as three P–O stretches in 1000–1200 cm^{-1} range, V=O stretch at 990–1000 cm^{-1}, P–O stretch at 975–985 cm^{-1}, as well as coupled V–O and P–O bending modes and skeletal vibrations in 150–600 cm^{-1} range. In addition, the Raman spectrum of vanadyl methylphosphonate is characteristic of P–C stretching mode at 786 cm^{-1}, and PO_3 bending modes at 538 and 426 cm^{-1}. Such similarities provide an additional support for the methylphosphonate/$VOHPO_4 \cdot 0.5H_2O$-type structure of vanadyl phosphite.

The infrared spectrum of vanadyl phosphite (Figure 3a and Table 2) exhibits a very sharp and strong peak at ca. 2439 cm^{-1} indicative of P–H linkages in the structure[14] and providing additional evidence for the phosphite structure. A number of symmetric and antisymmetric P–O stretching modes are observed in 1300–850 cm^{-1} range. The symmetric bending mode of PO_3 groups is seen at ca. 561 cm^{-1}. The 1617 cm^{-1} band corresponds to the bending mode of water molecules. Hydrogen bonding manifests itself in the strong and broad features at ca. 3600–2700 cm^{-1}. The band assignment in the IR spectrum of $VOHPO_4 \cdot 0.5H_2O$ shown in Figure 3b for comparison can be found elsewhere.[15]

(10) Wachs, I. E.; Segawa, E. In *Characterization of Catalytic Materials*; Wachs, I. E., Ed.; Butterworth-Heinemann: Boston, 1992; Chapter 4, p 71.
(11) Abdelouahab, F. B.; Olier, R.; Guilhaume, N.; Lefebvre, F.; Volta, J. C. *J. Catal.* **1992**, *134*, 151.
(12) Hardcastle, F.; Wachs, I. E. *J. Phys. Chem.* **1991**, *95*, 5031.
(13) Mount, R. A.; Raffelson, H. U.S. Patent 4,337,174, 1982.
(14) In *Phosphorus, an Outline of Its Chemistry, Biochemistry and Technology*; Corbridge, D. E. C., Ed.; Elsevier: Amsterdam, 1990; Chapter 14, p 1034.
(15) Johnson, J. W.; Johnston, D. C.; Jacobson, A. J.; Brody, J. F. *J. Am. Chem. Soc.* **1984**, *106*, 8123.

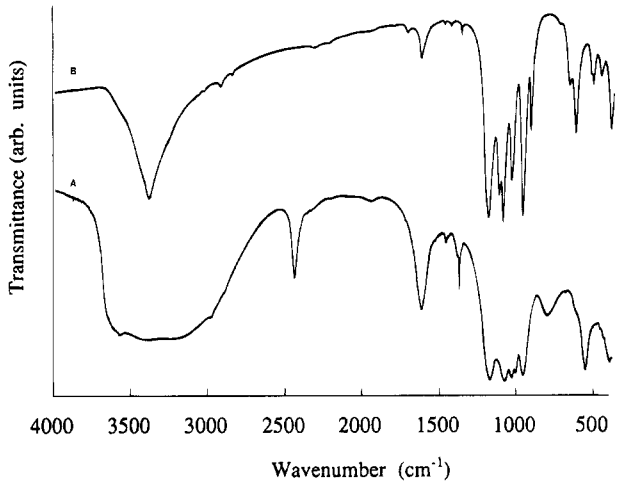

Figure 3. Infrared spectra of (A) $VOHPO_3 \cdot 1.5H_2O$ and (B) $VOHPO_4 \cdot 0.5H_2O$.

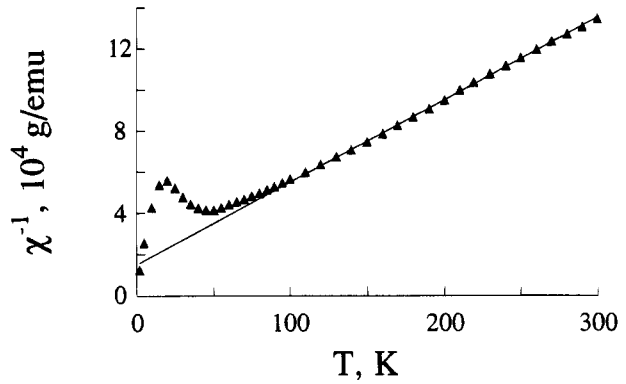

Figure 4. Inverse magnetic susceptibility of vanadyl phosphite vs temperature.

The proposed structure of vanadyl phosphite contains pairs of vanadyl octahedra which can exhibit antiferromagnetic exchange coupling at low temperatures. Such exchange interactions may be detected by magnetic susceptibility measurements. The plot of inverse susceptibility vs temperature for vanadyl(IV) phosphite is shown in Figure 4. The data in 150–300 K range are described very well by a Curie–Weiss behavior:

$$\chi_g = C_g/(T - \Theta) \quad (4)$$

where $C_g = 2.47 \times 10^{-3}$ emu·K/g is the Curie constant and $\Theta = -37.6$ K is the Weiss temperature. Deviation from linearity at $T < 150$ K in Figure 4 is due to short-range antiferromagnetic exchange interaction of paired vanadyls consistent with negative sign of the Weiss temperature. Johnson et al. assigned the initial increase in χ^{-1} at the very low temperatures, from 2 to 20 K in our case, to the presence of isolated paramagnetic centers.[15]

The TGA curve (10 K/min in air) of the vanadyl phosphite sample possessing the bulk $P/V = 0.85$ (Table 1) shows a multistep weight loss in 323–573 K range and weight gain in 573–973 K range (Figure 5b). For the stoichiometric conversion of vanadyl phosphite to vanadyl pyrophosphate:

$$2VOHPO_3 \cdot 1.5H_2O + O_2 = (VO)_2P_2O_7 + 4H_2O \quad (5)$$

a weight loss of 11.5% is expected, which is less than the 14.9% weight loss observed. This difference results from excess water adsorbed on the powdered sample as described above. Residual alcohol from the synthesis (ca. 1 wt %) is also lost below 573 K. Transformation to vanadyl pyrophosphate[7] is complete by 523 K (Figure 5b); temperatures at least 100–150 K higher are generally needed to convert $VOHPO_4 \cdot 0.5H_2O$ precursors into vanadyl pyrophosphate (Figure 5a). The weight gain peaks correspond to the process of further oxidation of vanadyl pyrophosphate into vanadyl(V) orthophosphate, $VOPO_4$, which takes place at higher temperatures. Formation of the latter phosphate was confirmed by the powder X-ray diffraction. The weight gain at higher temperatures (ca. 8.8%) agrees well with the complete oxidation of vanadyl(IV) pyrophosphate into vanadyl(V) orthophosphate (8.5% weight gain based on the results of Table 1):

$$(VO)_2P_2O_7 + {}^1/_2O_2 = 2VOPO_4 \quad (6)$$

Evidence of the layered structure of vanadyl phosphite comes from intercalation experiments. Solutions of primary *n*-alkylamines in nonaqueous solvents, such as anhydrous ethanol or *N,N*-dimethylacetamide were found to be suitable for intercalation of vanadyl phosphite, although the intercalated products were hydrolytically unstable in air.

After ca. 2 mol of amine were added per mole of vanadyl phosphite (the bulk P/V = 0.85), intercalated solids displayed low-angle peaks in the XRD patterns corresponding to expanded interlayer spacings. The interlayer spacings were found to linearly increase with the size of the alkyl group (Table 3 and Figure 6). Higher order reflections (up to fourth order) were observed in XRD. The linear relationship of the interlayer spacings with the number of carbon atoms n_c in

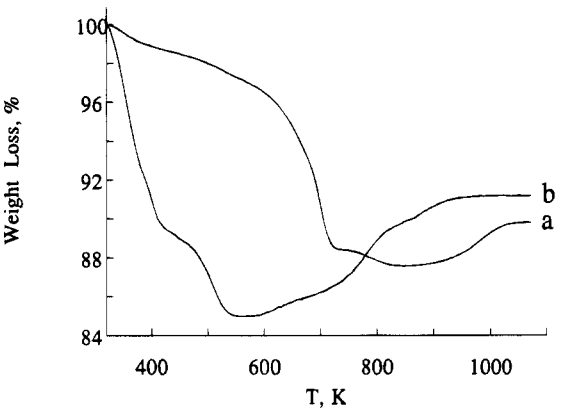

Figure 5. TGA curves of (a) $VOHPO_4 \cdot 0.5H_2O$ and (b) $VOHPO_3 \cdot 1.5H_2O$ in air. Heating rate: 10 K/min.

Table 3. *d* Spacings of Some $VOHPO_3 \cdot 1.5H_2O \cdot xRNH_2$ Phases (P/V = 0.85 Sample) Containing Monolayers of Intercalated Primary *n*-Alkylamines

n-alkylamine	*d* spacing, Å	*x* (C, H, N analysis)[a]	*x* (TGA in air)
n-hexylamine	12.66	0.64	0.65
n-heptylamine	13.75	0.60	0.60
n-octylamine	14.58	0.65	0.67
n-nonylamine	15.51	0.61	0.62
n-dodecylamine	17.83	0.53	0.54

[a] *n*-Hexylamine: 19.83% C, 5.22% H, 3.63% N. *n*-Heptylamine: 21.17% C, 5.39% H, 3.37% N. *n*-Octylamine: 24.43% C, 5.82% H, 3.55% N. *n*-Nonylamine: 26.61% C, 6.28% H, 3.35% N. *n*-Dodecylamine: 28.48% C, 6.58% H, 2.70% N.

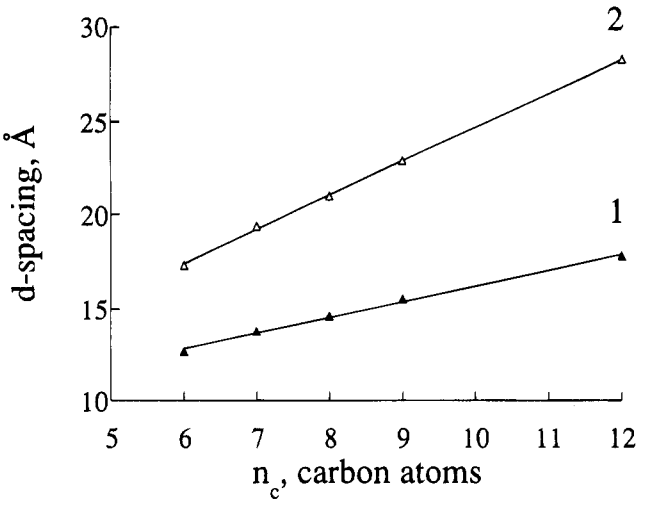

Figure 6. Interlayer spacings of $VOHPO_3 \cdot 1.5H_2O$ intercalated with some primary *n*-alkylamines vs the number of amine carbon atoms n_c, at low (1) and high (2) amine loadings.

Table 4. *d* Spacings of Some $VOHPO_3 \cdot 1.5H_2O \cdot xRNH_2$ Phases (P/V = 0.85 Sample) Containing Bilayers of Intercalated Primary *n*-Alkylamines

n-alkylamine	*d* spacing, Å	*x* (C, H, N analysis)[a]	*x* (TGA in air)
n-hexylamine	17.33	1.06	1.08
n-heptylamine	19.38	0.94	1.02
n-octylamine	20.96	1.07	1.14
n-nonylamine	22.84	0.90	0.94
n-dodecylamine	28.32	1.14	1.19

[a] *n*-Hexylamine: 27.31% C, 6.95% H, 5.18% N. *n*-Heptylamine: 28.18% C, 6.93% H, 4.53% N. *n*-Octylamine: 33.16% C, 7.76% H, 4.85% N. *n*-Nonylamine: 32.36% C, 7.54% H, 4.11% N. *n*-Dodecylamine: 42.81% C, 8.84% H, 4.12% N.

amine molecule (Figure 6) is given by the following expression:

$$d = 7.72 + 0.85n_c \text{ (Å)} \quad (7)$$

At higher amine loadings (addition of ca. 6 mol of amine/mol of vanadyl phosphite), a set of intercalated compounds was obtained (Table 4) where the *d* spacings also increased linearly with the size of the alkyl group according to eq 8:

$$d = 6.49 + 1.82n_c \text{ (Å)} \quad (8)$$

These two amine loadings have been assigned to intercalated amine mono- and bilayer structures, respectively (vide infra). The extreme hydrolytic sensitivity of the intercalated phases made their isolation and analysis very difficult.

Discussion

A new layered $V^{IV}-P^{III}$ phosphate, vanadyl phosphite, or $VOHPO_3 \cdot 1.5H_2O$, has been synthesized. On the basis of XRD, elemental analysis, vibrational spectroscopy, magnetic susceptibility, and intercalation of *n*-alkylamines, we suggest this compound to be structurally similar to $VOHPO_4 \cdot 0.5H_2O$.

Johnson et al. synthesized a number of vanadyl organophosphonates and characterized their structures.[6] They concluded that the ability of the system to crystallize in either corner-sharing (e.g., vanadyl phenylphosphonate[16]) or face-sharing vanadyl octahedra type structure (i.e., $VOHPO_4 \cdot 0.5H_2O$[15]) is determined by the packing constraints of the organo group attached to phosphorus on the phosphonate layer.[6a]

Table 5. X-ray Diffraction Data for Vanadyl Phosphite[a]

hkl	d_{obs}	d_{calc}	I_{obs}
010	7.268	7.237	100
011	5.746	5.752	5
111	4.360	4.354	11
020	3.617	3.618	5
200	3.318	3.331	12
013	2.892	2.896	72
203	2.293	2.292	8
204	1.930	1.931	6
303	1.819	1.817	17
040	1.809	1.809	5

[a] Possible orthorhombic space group; $a = 6.661$ Å, $b = 7.237$ Å, $c = 9.480$ Å; $\lambda = 1.5405$ Å.

Assuming that vanadyl phosphite layer has essentially the same structure as $VOHPO_4 \cdot 0.5H_2O$ and thus the unit-cell layer area of ca. 71 Å^2 and the number of formula units per unit cell, Z, is 4, then four P–H hydrogen atoms would require only $4 \times 7.45 = 29.8$ Å^2. Therefore it is clear that the hydrogen atoms do not impose any packing constraints on the layer and vanadyl phosphite could crystallize in the $VOHPO_4 \cdot 0.5H_2O$-type structure.

Johnson et al. have recently reported partial structure solution of the layered vanadyl methylphosphonate ($VOCH_3PO_3 \cdot 1.5H_2O$) which indicated apparent monoclinic structure (space group $P2_1/a$) and V–P–O connectivity similar to $VOHPO_4 \cdot 0.5H_2O$.[14] On the basis of the above-mentioned considerations of packing constraints in vanadyl phosphonates, vanadyl phosphite should have the V–P–O connectivity analogous to $VOHPO_4 \cdot 0.5H_2O$ or $VOCH_3PO_3 \cdot 1.5H_2O$. In vanadyl phosphite the $V_2O_8(H_2O)$ dimers would be connected through corners by the HPO_3 tetrahedra. Hydrogen atoms belonging to phosphite tetrahedra are extended out from both sides of the layer. Intercalated water molecule is probably hydrogen-bonded to vanadyl oxygens in adjacent layers, ultimately controlling the packing of the layers relative to one another in an orthorhombic or monoclinic unit cell and resulting in the interlayer spacing of 7.27 Å. Unfortunately, we have not been able yet to obtain crystals of sufficient quality to attempt to solve the structure by single-crystal or powder XRD methods. A refinement of the XRD pattern with both orthorhombic and monoclinic cells was carried out. The best fit orthorhomic structure for the powder XRD pattern of vanadyl phosphite has been tentatively indexed with $a = 6.66$, $b = 7.24$, and $c = 9.48$ Å, as shown in Table 5. The small number of reflections in powder XRD pattern of vanadyl phosphite and their broadness (Figure 1) do not permit more definitive choice of the unit cell. The in-plane unit lattice parameters are similar to those of $VOHPO_4 \cdot 0.5H_2O$, while the interlayer spacing is expanded relative to $VOHPO_4 \cdot 0.5H_2O$. The XRD pattern could also be fit with a monoclinic cell with $a = 14.00$, $b = 4.05$, $c = 7.53$ Å, and $\beta = 106°$; however, the b value for this structure is physically unreasonable, and so we felt the orthorhombic structure is more reasonable. We stress

(16) Huan, G.; Jacobson, A. J.; Johnson, J. W.; Goshorn, D. P. *Chem. Mater.* **1992**, *4*, 661.

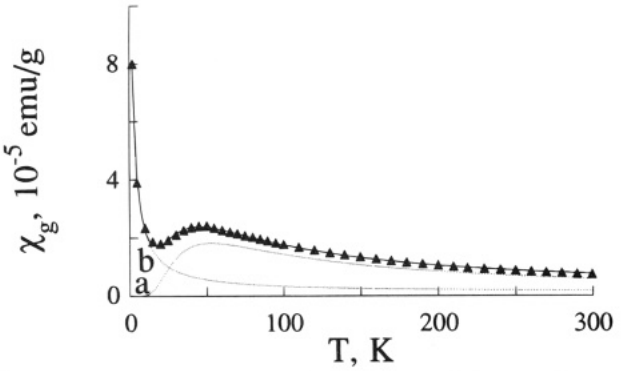

Figure 7. Magnetic susceptibility of vanadyl phosphite vs temperature. Dotted lines represent the contribution of (a) vanadyl dimers and (b) isolated paramagnetic centers.

Table 6. Magnetic Susceptibility Parameters for Vanadyl Phosphite and $VOHPO_4 \cdot 0.5H_2O$

parameters	vanadyl phosphite	$VOHPO_4 \cdot 0.5H_2O$[15]
C_g, emu·K/g	2.46×10^{-3}	2.08×10^{-3}
Θ_g, K	−37.6	−25.3
χ_o, emu/g	10^{-6}	-3×10^{-7}
C_i, emu·K/g	2.4×10^{-4}	4.0×10^{-5}
C_d, emu·K/g	1.90×10^{-3}	2.12×10^{-3}
J, cm^{-1}	−29.4	−30.6
$\Theta = J/2k_B$, K	−21	−22
μ_{eff}	$1.73\mu_B$	$1.72\mu_B$

that these structural assignments are only our best guess based on the limited quality of the XRD data, and additional evidence from magnetic susceptibility and spectroscopic data.

When larger benzyl alcohol molecule was used during the synthesis of vanadyl phosphite, a solid with a different powder XRD pattern was produced. This seems to be in agreement with previous observation in case of vanadyl methylphosphonate when the structure with corner-sharing vanadyl octahedra apparently resulted to accommodate larger alcohol molecule in the coordination sphere of vanadyl(IV) ions.[17] This observation stresses the importance of alcohol molecules as templates in the synthesis of vanadyl phosphonates. The size of an alcohol molecule controls the type of V−P−O connectivity in case of vanadyl phosphonates and the morphology of $VOHPO_4 \cdot 0.5H_2O$ precursor. In the latter case, the strong interlayer hydrogen bond network probably defines the V−P−O connectivity and formation of vanadyl dimer structure.

The magnetic susceptibility data (Figure 7) show no departure from Curie−Weiss behavior until lower temperatures (ca. 150 K), where the behavior of vanadyl phosphite is similar to that of $VOHPO_4 \cdot 0.5H_2O$ and indicates the presence of exchange-coupled vanadyl dimers. The data were analyzed using the expression for an isolated dimer model containing two $S = 1/2$ cations with isotropic g tensor:[16]

$$\chi = \chi_0 + C_i/(T - \Theta) + 4C_d/(T(3 + \exp(-2J/k_BT))) \quad (9)$$

Least-squares fits to the data over the entire temperature range are also shown in Figure 7. Values of χ_0, the temperature independent contribution; C_d, the Curie constant associated with the vanadyl dimers; C_i and Θ, the constants associated with the magnetic impurities;

Monoclinic Cell: a=8.68, b=5.75, c=7.76Å, β=110.7°

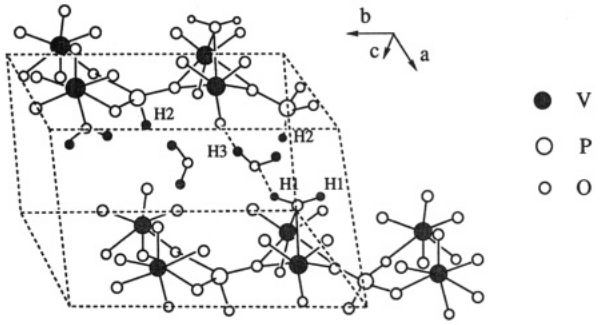

Figure 8. Proposed V−P−O connectivity in $VOHPO_3 \cdot 1.5H_2O$ in the *ac* plane. Dashed lines represent the unit lattice in the *ab* plane. Only half of the nonstructural water molecules are shown. Hydrogen bonds between oxygen (black circles) and hydrogen atoms (light circles) are indicated by short dashed lines.

and J, the coupling constant within the vanadyl pairs are reported in Table 6 along with the data for $VOHPO_4 \cdot 0.5H_2O$.[15] These results are also consistent with the magnetic susceptibility data for C_1−C_3 phosphonates.[17] The contributions of the vanadyl dimers and isolated paramagnetic centers are shown in Figure 7 as the dotted lines. If V(IV) defects are assumed to be those isolated paramagnetic centers, then the ratio of isolated to paired V=O is $C_i/C_d = 12.4\%$. The very small size of crystallites in vanadyl phosphite (ca. 15 nm on the basis of the Scherrer equation) as seen in X-ray diffraction and transmission electron microscopy experiments, and the presence of V(IV) defects at the surface of the crystallites can account for the deviation of $C_g = 2.47 \times 10^{-3}$ emu·K/g obtained above from the fit to the eq 1 from $C_i + C_d = 2.14 \times 10^{-3}$ emu·K/g. From $C_i + C_d$, the effective moment per V(IV) ion is found to be $\mu_{eff} = 1.73\mu_B$, which is identical with the value expected for a spin $1/2$ ion with $g = 2$. Therefore, the magnetic susceptibility data are consistent with the structure of vanadyl phosphite in which weakly exchange-coupled vanadyl dimers (-29.4 cm^{-1}) are effectively isolated from each other as is the case in $VOHPO_4 \cdot 0.5H_2O$.[15] Leonowicz et al. proposed a model of hydrogen bonding in $VOHPO_4 \cdot 0.5H_2O$.[18] According to this model, P−OH group is involved in the strong hydrogen bonding to vanadyl oxygens and structural water protons making this structure much more resistant to intercalation than other layered hydrogen phosphates.[19] On the basis of the structural analogy with $VOHPO_4 \cdot 0.5H_2O$, we expect water to occupy all available layer area, i.e., ca. 71 − 29.8 = 41.2 Å^2. Taking the van der Waals area of water molecule as ca. 39 Å^2, up to one crystallization water molecule (not to be confused with the structural water) is expected per close-packed unit cell layer of $VOHPO_4 \cdot 0.5H_2O$-like structure, which is indeed confirmed by the results of elemental analysis of vanadyl phosphite. Such water molecules may form a network of hydrogen bonds between the vanadyl oxygens in adjacent layers shown in Figure 8.

Weaker interlayer hydrogen bonding in vanadyl(IV) phosphite as compared to $VOHPO_4 \cdot 0.5H_2O$ makes the

(17) Huan, G.; Johnson, J. W.; Brody, J. F.; Goshorn, D. P. *Mat. Chem. Phys.* **1993**, *35*, 199.

(18) Leonowicz, M. E.; Johnson, J. W.; Brody, J. F.; Shannon, H. F., Jr.; Newsam, J. M. *J. Solid State Chem.* **1985**, *56*, 370.

(19) Guliants, V. V.; Benziger, J. B.; Sundaresan, S. *Chem. Mater.* **1994**, *6*, 353.

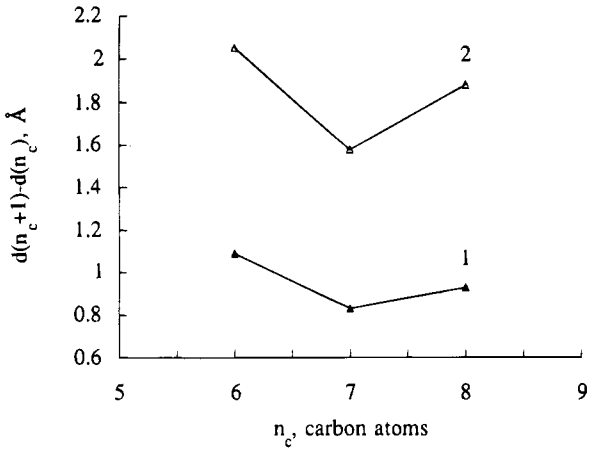

Figure 9. Interlayer spacing changes in the intercalated vanadyl phosphite containing amine monolayers (1) and bilayers (2) as a function of n_c.

former more amenable to intercalation of guest molecules. *n*-Alkylamines containing up to 12 carbon atoms were directly intercalated into vanadyl phosphite, whereas amines with more than 5 carbon atoms would not intercalate into $VOHPO_4 \cdot 0.5H_2O$ directly.[19]

In the first set of intercalated compounds obtained at low amine loadings the interlayer spacings increase on average by 0.85 Å/carbon atom in the amine molecule (Figure 6). In the case of straight *trans,trans*-alkyl chain, an increase of alkyl chain length is estimated to be Δl = 1.27 Å/carbon atom; the 0.85 Å increase indicates that the amine molecules are arranged as monolayers tilted at arcsin{0.85/1.27} = 42.0° relative to the layers of vanadyl phosphite. This tilt angle is smaller than the reported values of tilt angles in other layered phosphates: 59.6° in $VOHPO_4 \cdot 0.5H_2O$,[19] 58.7° in α-TiP, 54.2° in α-ZrP, and 66.0° in α-SnP.[20] The value of the tilt angle indicates that the N−C bond is not strictly perpendicular to the phosphite layers (53.8° for perpendicular arrangement).

In fully intercalated compounds, the *d*-spacing increase of 1.82 Å/carbon atom in amine molecule exceeds the value of 1.27 Å/carbon atom for a single *trans,trans*-alkyl chain. Such a *d*-spacing increase corresponds to a double-layer arrangement of amine molecules tilted at arcsin{1.82/(2·1.27)} = 45.7°.

The change in interlayer spacing when going from an n_c to $n_c + 1$ compound depends on whether n_c is even or odd as shown in Figure 9. The alternating small and large changes in the interlayer spacings shown in Figure 9 suggest that the N−C bond is nearly perpendicular to the phosphite layer, so that the terminal C−C bond makes a smaller or larger angle relative to the layer depending on n_c (Figure 10). Assuming the N−C bond perpendicular to the layer, tetrahedral bond angles and a C−C bond length of 1.54 Å, the $d(n_c) - d(n_c + 1)$ for amine bilayers is expected to be 1.01 Å (n_c is odd), and 3.08 Å (n_c is even), or 0.51 and 1.54 Å for odd and even n_c, respectively, in the case of amine monolayers.[20] The *d*-spacing changes in the vanadium phosphite system (Figure 9) are less pronounced, which is explained by a smaller tilt angle than expected for perpendicular orientation of the N−C bond relative to the phosphite layers.

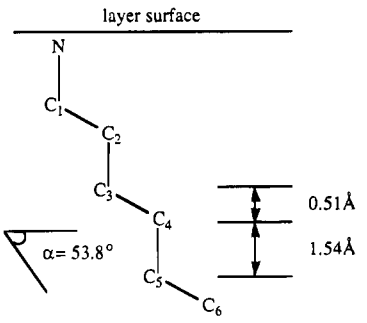

Figure 10. Hypothetical arrangement of *n*-hexylamine in the interlayer space corresponding to the N−C bond perpendicular to the layer surface.

The values of the tilt angle in intercalated vanadyl phosphite phases smaller than those in intercalated hydrogen phosphates[19,20] may indicate a different bonding environment. In fact, since the −PH groups present on the phosphite layer are rather nonpolar, we suggest that only structural and intercalated water molecules would participate in hydrogen bonding with primary *n*-alkylamine. The extrapolated interlayer spacing at $n = 0$ for the bilayer of intercalated amines is reduced relative to the monolayer (6.49 vs 7.72 Å) which may also indicate partial deintercalation of water.

The "space-filling" model[20] can be applied to vanadyl phosphite to estimate the efficiency of the amine packing in the interlayer space. We assume that (i) the inlayer structure of vanadyl phosphite is similar to that of $VOHPO_4 \cdot 0.5H_2O$,[18] (ii) the intercalated amine is only hydrogen-bonded to structural water molecules, and (iii) the contribution of the amino groups is the same for all amines. The packing density of the alkyl chains in the interlayer space (V_p) given by:

$$V_p = V_c/V_t \tag{10}$$

$$V_c = yNV_a = yNn_c\Delta l\sigma \text{ (cm}^3\text{)} \tag{11}$$

where V_c and V_t are the alkyl chain volume and the interlayer space volume per unit area of layer surface, e.g., 1 cm^2, respectively; y, the average number of amine molecules per acid site on the layer, is equal to $2x$ based on the theoretical $VOHPO_3 \cdot H_2O \cdot (0.5H_2O)_{struct} \cdot xRNH_2$ composition (Tables 3 and 4); $N \approx 2.9 \times 10^{14}$, the surface density of structural water molecules per cm^2 of the hypothetical $VOHPO_3 \cdot 1.5H_2O$ layer (Table 5), V_a is the volume of an individual amine molecule, $n_c\Delta l$, the length of the hydrocarbon chain and $\sigma = 18.6 \times 10^{-16}$ cm^2, the cross-section area of a *trans,trans*-alkyl chain (found from the *a* and *b* unit-cell parameters of crystalline $C_{29}H_{60}$[21]). All interlayer space apart from the region occupied by the phosphite layer with protonated amino groups is available to alkyl chains. The available volume V_t per 1 cm^2 of layer surface is

$$V_t = d - d^\circ \text{ (cm}^3\text{)} \tag{12}$$

where d°, the combined height of the phosphate layer and amino groups, is assumed to be independent of n_c and equal to the extrapolated value of d for $n_c = 0$.

To estimate the packing density of amines in the interlayer space of vanadyl phosphite, we have substi-

(20) Menéndez, F.; Espina, A.; Trobajo, C.; Rodríguez, J. *Mater. Res. Bull.* **1990**, *25*, 1531.

(21) Kitaigorodsky, A. I. *Molecular Crystals and Molecules*; Academic Press: New York, 1973.

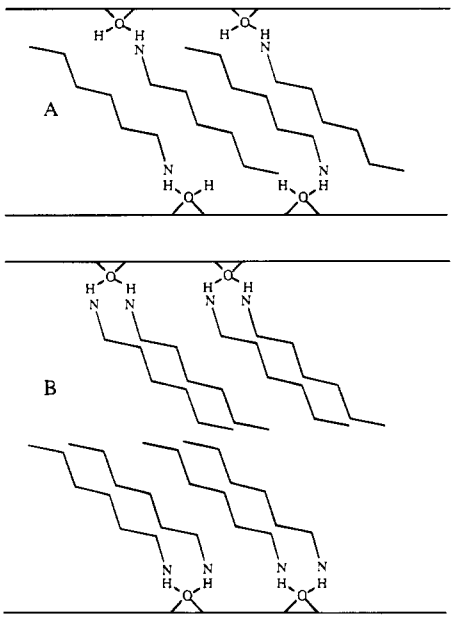

Figure 11. Proposed arrangement of primary *n*-alkylamines in the interlayer space of vanadyl phosphite: (A) monolayers; (B) bilayers.

tuted linear fits $d = d^\circ + \delta n_c$ from eqs 7 and 8 into eq 12, and combined it with eqs 11 and 10 to obtain

$$V_p = yN\Delta l\sigma/\delta \ (\mathrm{cm}^3) \qquad (13)$$

where δ is the slope in eqs 7 and 8. Using average values of $x = 0.61$ and 1.02 (Tables 3 and 4) for the two sets of intercalated vanadyl phosphites gave average packing densities of ca. 1.0 and 0.8 for the amine mono- and bilayer compounds, respectively. The value of 1.0 obtained in the former set of compounds is consistent with close-packing of intercalated amines on the phosphite layer.[20] On the other hand, the observed close-packing of amines supports the structural similarity between $VOHPO_4 \cdot 0.5H_2O$ and vanadyl phosphite, as well as suggesting that the structural water present in the $VOHPO_4 \cdot 0.5H_2O$-type solids is involved in hydrogen bonding.[19] Somewhat lower packing density of amine bilayers in the fully intercalated compounds (ca. 0.8) may indicate a different hydrogen bonding environment. In fact, a decrease in the thickness of the phosphite layer (6.49 vs 7.72 Å) in fully intercalated vanadyl phosphite may result from the displacement of the intercalated water coordinated to the phosphite layer by amine molecules into the interlayer space leading to the observed lower packing density of the alkyl chains. The proposed arrangement of alkylamines in the interlayer space of vanadyl phosphite is shown in Figure 11.

Conclusions

A new layered V(IV)–P(III) phosphate, vanadyl phosphite ($VOHPO_3 \cdot 1.5H_2O$), has been synthesized and characterized by a number of methods, including powder XRD, magnetic susceptibility measurements, Raman spectroscopy, infrared spectroscopy, thermogravimetric analysis, and *n*-alkylamine intercalation. The powder XRD and Raman results indicate that vanadyl phosphite can be obtained essentially as a single-phase material, while the low-temperature behavior of magnetic susceptibility indicates antiferromagnetic coupling and thus the presence of vanadyl dimers in its structure. On the basis of the experimental data obtained, a structure of vanadyl phosphite is proposed, in which vanadyl dimers $V_2O_8(H_2O)$ are connected through the phosphite tetrahedra within the layers. The hydrogen atoms on phosphite groups are directed toward the interlayer space and additional water molecules are intercalated forming the hydrogen-bond network between vanadyl oxygens in adjacent layers. These water molecules probably determine packing of the layers relative to one another, and eventually the symmetry of the unit cell (possibly orthorhombic).

Weaker interlayer hydrogen bonding in vanadyl phosphite as compared to $VOHPO_4 \cdot 0.5H_2O$[19] makes the former much more amenable to intercalation of guest molecules, e.g., primary *n*-alkylamines. Besides, vanadyl pyrophosphate catalysts produced from vanadyl phosphite have been found to have higher surface areas and higher selectivities to maleic anhydride in partial oxidation of *n*-butane at higher *n*-butane conversions than conventional organic catalysts.[7]

Acknowledgment. We thank Dr. K. Chary of Rutgers University for the magnetic susceptibility measurements, Dr. J. M. Jehng and Professor I. E. Wachs (Lehigh University) for the Raman spectra, and Drs. J. M. Forgac, M. S. Haddad, and G. W. Zajac (AMOCO Chemical Corp.) for the XPS data, and Dr. F. Scheidl (Robertson Microlit Laboratories, Inc.) for discussions of the elemental analysis. This work was supported by the AMOCO Chemical Corp. and National Science Foundation Grant CTS-9100130.

CM950007T